Aberrant Splicing in the *PKD2* Gene as a Cause of Polycystic Kidney Disease

DAVID M. REYNOLDS,* TOMOHITO HAYASHI,* YIQIANG CAI,* BARBERA VELDHUISEN,† TERRY J. WATNICK,‡ XOSE M. LENS,§ TOSHIO MOCHIZUKI,* FENG QIAN,‡ YOSHIKO MAEDA,* LI LI,* RAGNHEIDUR FOSSDAL,‖ ELIECER COTO,¶ GUANQING WU,* MARTIJN H. BREUNING,† GREGORY G. GERMINO,‡ DORIEN J. M. PETERS,† and STEFAN SOMLO*

**Departments of Medicine and Molecular Genetics, Albert Einstein College of Medicine, Bronx, New York; †Department of Human Genetics, Sylvius Laboratory, Leiden University, Leiden, Netherlands; ‡Department of Medicine, Johns Hopkins University School of Medicine, Baltimore, Maryland; §Complexo Hospitalario, Universitario de Santiago, Santiago de Compostela, Spain; ‖Department of Medical Genetics, National University Hospital, Reykjavik, Iceland; ¶Servicio de Immunologia, Hospital Central de Asturias, Oviedo, Spain.*

Abstract. It is estimated that approximately 15% of families with autosomal dominant polycystic kidney disease (ADPKD) have mutations in *PKD2*. Identification of these mutations is central to identifying functionally important regions of gene and to understanding the mechanisms underlying the pathogenesis of the disorder. The current study describes mutations in six type 2 ADPKD families. Two single base substitution mutations discovered in the ORF in exon 14 constitute the most COOH-terminal pathogenic variants described to date. One of these mutations is a nonsense change and the other encodes an apparent missense variant. Reverse transcription-PCR from patient lymphoblast RNA showed that, in addition, both mutations resulted in out-of-frame splice variants by activating cryptic splice sites via different mechanisms. The apparent missense variant produced such a strong splicing signal that the processed transcript from the mutant chromosome did not contain any of the normally spliced, missense product. A third mutation, a nonconservative missense change effecting a negatively charged residue in the third transmembrane span, is likely pathogenic and defines a highly conserved residue consistent with a potential channel subunit function for polycystin-2. The remaining three mutations included two frame shifts resulting from deletion of one or two bases in exons 6 and 10, respectively, and a nonsense mutation due to a single base substitution in exon 4. The study also defined a novel intragenic polymorphism in exon 1 that will be useful in analyzing "second hits" in *PKD2*. Finally, the study demonstrates that there are reduced levels of normal polycystin-2 protein in lymphoblast lines from PKD2-affected individuals and that truncated mutant polycystin-2 cannot be detected in patient lymphoblasts, suggesting that the latter may be unstable in at least some tissues. The mutations described will serve as critical reagents for future functional studies in *PKD2*.

The identification of mutations in human disease genes, especially those that encode proteins of unknown function, can be instructive for identification of functionally important domains and can serve as guideposts for experimental investigation into the pathogenesis of disease. Almost all cases of autosomal dominant polycystic kidney disease (ADPKD) result from mutations in either *PKD1* or *PKD2*. *PKD1* and *PKD2* encode integral membrane proteins whose functions remain unknown. Mutations in *PKD2* occur less frequently (1) and manifest with a less severe form of ADPKD (2,3) than mutations in *PKD1*. *PKD2* is encoded in at least 15 exons spanning approximately 68 kb on chromosome 4q21–23 (4). Exons 2 to 14 are amenable to mutation detection by single-strand conformational analysis (SSCA) using intronic primers flanking 3′ and 5′ splice sites. This approach is suitable for detecting sequence variation within the coding region and in intronic regions, including splice sequences, immediately flanking the exons (4). Exon 1 is at least 660 bp and very GC-rich and is therefore best amplified for SSCA in three overlapping segments (4).

Polycystin-2, the *PKD2* gene product, is a widely expressed integral membrane glycoprotein (5) with structural similarity to cation channel subunit proteins. A polycystin-2 homolog has been identified (6,7), and proteins with structural similarity, including polycystin-1, have been found in several lower multicellular organisms (5,8,9). Polycystin-2 interacts with polycystin-1 via its cytoplasmic COOH-terminal domain, and naturally occurring human mutations have been shown to interfere with this function (10,11). It has been postulated that the polycystins participate in a cellular signaling pathway, with

Received March 26, 1999. Accepted May 12, 1999.
Correspondence to Dr. Stefan Somlo, Section of Nephrology, Yale University School of Medicine, LMP 2073, 333 Cedar Street, New Haven, CT 06520-8029. Phone: 203-785-7595; Fax: 203-624-8213; E-mail: stefan.somlo@yale.edu
1046-6673/1011-2342
Journal of the American Society of Nephrology

polycystin-1 acting as a receptor that modulates the activity of polycystin-2. Polycystin-2 contains an EF hand and several putative phosphorylation sites in the COOH terminus (5).

Thirty-seven mutations in *PKD2* have been described in the literature (5,12–16). Mutations have been found throughout the gene, although no mutations have been reported in exons 9, 10, 14, and 15. The majority of mutations have been premature chain terminations due to nonsense codons, frame shifting oligo-bp insertions/deletions, or splice site mutations with altered reading frames. No clustering of mutations has been described and only a few mutations have been found to occur in more than one family. One missense variant has been implicated as a pathogenic change (14).

One intragenic polymorphism has been identified by SSCA (14). Cyst formation in both forms of polycystic kidney disease is thought to occur by a "two-hit" mechanism (17–19). Loss of heterozygosity at intragenic polymorphic loci in human tissues has been used to demonstrate this mechanism in type 1 ADPKD (17,18,20), while the evidence in type 2 ADPKD comes from an animal model (19). Second hits may explain the intrafamilial variation in disease presentation and may account for the apparent absence of genotype/phenotype correlation in type 2 ADPKD (12).

In the current study, we report screening for mutations in the entire coding sequence of *PKD2* in 12 families, with the identification of mutations in six of them. Two mutations were found in exon 14 and constitute the most COOH-terminal pathogenic variants described to date. One mutation is a missense change that is likely pathogenic and defines a highly conserved residue of potential functional importance. In a pair of families, we examine the transcriptional consequence of the genomic mutations and demonstrate two separate mechanisms of cryptic splice site activation. We define a novel intragenic polymorphism that will be useful in analyzing "second hits" in *PKD2*. Finally, we demonstrate the occurrence of reduced levels of polycystin-2 protein expression in lymphoblast lines from affected individuals.

Materials and Methods

Family Selection and DNA/RNA Preparation

Twelve ADPKD families with either demonstrable linkage to *PKD2* markers or exclusion of linkage to *PKD1* markers were screened for mutations in *PKD2*. At-risk individuals participating in this study were examined by ultrasonography (21). DNA from one affected individual of each family was selected for SSCA (see below). DNA was isolated from blood leukocytes or Epstein-Barr virus (EBV)-transformed lymphoblasts using the Puregene DNA isolation kit (Gentra Systems, Research Triangle Park, NC). RNA was isolated from lymphoblast cell lines of ADPKD4, PK9505, and controls using TRIzol reagent (Life Technologies, Gaithersburg, MD). Reverse transcription (RT)-PCR template was produced using SuperScipt II (Life Technologies), according to the manufacturer's recommendations. Mutations were found in families collected in the United States (ADPKD4), The Netherlands (PK5147, 5109), Spain (family 9, Oviedo 23), and Iceland (PK9505).

SSCA and Identification of Mutations and Polymorphisms

Oligonucleotide primers complementary to intronic sequences flanking exons 2 to 14 (4) were used to amplify the exons and adjacent splice junction sites of the *PKD2* gene. Exon 1 was amplified in three overlapping fragments of 248, 249, and 210 bp, because the entire coding region of the exon is too large for efficient SSCA and it cannot be reliably amplified due to GC richness (4). Only the ORF portion of exon 15 was analyzed by SSCA (4). Amplification was performed using 20 to 50 ng of template DNA under conditions as described previously (4). The mutation in ADPKD4 was initially detected in RT-PCR products from lymphoblast RNA and then screened in genomic DNA; all other variants were initially detected in genomic DNA. The PK9505 mutation was further analyzed by RT-PCR in cDNA from lymphoblasts and has been used in studies of PKD2 protein interactions (10). The PCR primers used in this study were those described previously (4), in addition to primers shown in Table 1.

SSCA was performed as described previously (5). One affected individual from each of the 12 families and two unrelated, healthy control subjects comprised the screening panel. All samples were run under at least two different gel conditions. Exons exhibiting aberrantly migrating SSCA fragments were reamplified, and PCR products were gel-purified using the QIAquick kit (Qiagen, Santa Clarita, CA).

Table 1. Primers used for detection of mutations and polymorphism

Exon	Primer Pair	Sequence (5′ → 3′)[a]	Size (bp)	T_m (°C)
1	1bpoly2F	TGA GCT CCG TGG GCG CGC GGA GCC **t**G**a** G	111	72[b]
	R49	CTG GGC TGG GGC ACG GCG GG		
6	6*Bsp*F1/IR8[c]	CAG GAG TTT CTG GAA TTG TC**c** G	84	55
13–15	F12	TAG TGG CGT TTC TTA CGA AG	243[d]	55
	R12	TCT TCA CGT ACT AGC CGT TC		
14–15	F17/R12	ATT CCA TCG GCA GCA TAG	684	55

[a] Lower case, bold, underlined bases differ from the sequence in GenBank accession (U50928) and are designed to introduce restriction sites into the amplification products (Table 2).

[b] Amplification of this product in the GC-rich exon 1 requires use of the r*Tth* DNA polymerase XL (Perkin Elmer, Norwalk, CT).

[c] The primer sequence for IR8 is published (4).

[d] This is the product size when these primers are used to amplify cDNA template; in genomic DNA, these primers would amplify across introns 13 (>5 kb) and 14 (499 bp).

Products were sequenced in both directions by cycle sequencing using the PCR primers and dye terminator chemistries on an ABI 377 Prism automated sequencer. Heterozygous variants were identified as double peaks in the sequence electropherogram. Variants were taken to be pathogenic mutations if the sequence changes clearly resulted in premature termination of the putative translation product. Evidence for the latter was obtained in genomic DNA for PK5147, Oviedo 23, PK5109, and PK9505 and from RNA for ADPKD4 and PK9505. In the case of the missense variant, the occurrence of a nonconservative codon change that exclusively segregated with the disease phenotype (family 9) and was not observed in 101 normal chromosomes and 11 other affected chromosomes was taken as proof of pathogenicity. Sequence changes observed in affected and normal chromosomes constituted polymorphisms.

The nucleotide location of mutations in the cDNA sequence (GenBank accession no. U50928) is designated with the A in the initiation codon as base number 1. Codons are designated with the initiation codon as number 1.

Restriction Enzyme Analysis

The mutation in family PK5147 created an *Nla*III site and the mutation in PK9505 destroyed a *Cac*8I site. The mutation in family 9 and the exon 1 polymorphism did not alter naturally occurring restriction sites. To address this, primers were designed that incorporated one or two nucleotide sequence alterations, respectively, to introduce restriction sites into the published sequence (GenBank accession no. U50928) that are absent in the variant sequences (Table 1). PCR amplification was performed in triplicate 50-μl reactions at annealing temperatures shown in Table 1, and the PCR products were purified using the QIAquick kit and eluted in a 50-μl final volume. Restriction digests were performed in 25-μl reactions containing 15 μl of eluted PCR products, 15 units of enzyme, and the buffer recommended by the manufacturer (New England Biolabs, Beverly, MA). Digests were visualized by ethidium bromide staining after separation on agarose or polyacrylamide gels.

Antibodies Immunoblotting and Glycosylation Analysis

The production and characterization of the YCC2 and YCB9 antisera are described elsewhere (19) (Y. Cai, unpublished data). Briefly, fusion proteins C2 (amino acids 687 to 962) and B9 (amino acids 103 to 203) containing most of the cytoplasmic COOH- and NH_2-terminal portions of polycystin-2, respectively, were produced by subcloning PCR-generated fragments of the *PKD2* cDNA into the pGEX2T expression vector (Pharmacia Biotech, Piscataway, NJ). The fusion proteins were expressed in bacteria and purified with glutathione-agarose before being used to immunize New Zealand rabbits to raise polyclonal antisera (HRP, Inc., Denver, PA). The specificities of both antisera have been confirmed by immunoblotting, immunoprecipitation, peptide competition, and cell transfection studies (19) (Y. Cai, unpublished data).

For immunoblot analysis of lymphoblast protein, 20 to 150 μg of membrane fraction protein obtained after 100,000 $\times$ *g* centrifugation of a precleared lysate was solubilized in sample buffer (125 mM Tris, pH 6.8, 200 mM dithiothreitol, 6% sodium dodecyl sulfate [SDS], 20% glycerol, and 0.2% bromphenol blue) and separated by electrophoresis on 5 or 8% SDS-polyacrylamide gel electrophoresis gels without boiling. Fractionated proteins were electrotransferred to Polyscreen polyvinylidene difluoride membranes (Du Pont/New England Nuclear, Boston, MA) and detected with the YCC2 (1:5000) or YCB9 (1:1000) polyclonal antisera, using ECL enhanced chemiluminescence (Du Pont/New England Nuclear).

Membrane fraction protein was treated with endoglycosidase H (Endo H) following the manufacturer's protocols (New England Biolabs). Reactions were incubated at 37°C overnight with 1 μl (500 U) of Endo H in the appropriate buffer in 20 to 40 μl of total reaction volume. After the overnight incubation, an equal volume of 2$\times$ SDS sample buffer was added to each reaction, and incubated at 37°C for 30 min before SDS-polyacrylamide gel electrophoresis and immunoblot analysis.

Results

Intron-based PCR primers were used to screen all 15 exons of the *PKD2* gene in 12 families with non-PKD1 forms of ADPKD. Six variants (50%) were identified that are likely to be pathogenic in this group (Table 2). All six variants are distinct from each other and five are novel.

Nonsense Mutations

The mutations in PK5147 and PK9505 in exons 4 and 14, respectively, are C to T transitions in arginine codons producing TGA stop codons (Table 2). The mutation in PK5147 introduces an *Nla*III restriction site, and digestion of exon 4 PCR products with this enzyme demonstrates segregation of this mutation with the disease phenotype in this family (Figure 1).

The mutation in PK9505 is the first found in exon 14, occurring 35 codons downstream of any previously reported mutation. The single base change results in loss of a *Cac*8I restriction site, and this feature has been used to confirm that the genomic mutation segregates with the disease phenotype in the PK9505 family (data not shown). Analysis of lymphoblast RNA from an affected individual by RT-PCR, however, suggests a more complex mechanism for this mutation. In addition to the expected 243-bp RT-PCR product generated with primers F12/R12 (Table 1), a smaller RT-PCR product is also observed (Figure 2). RT-PCR from unaffected lymphoblast cell lines produce only the 243-bp product. Sequencing of the 243-bp product from PK9505 revealed heterozygosity at nucleotide 2614, with both the wild-type (C) and nonsense mutation (T) identified in the transcript. Sequencing of the same product from healthy individuals revealed only the wild-type sequence. The heterozygous nature of the PK9505 transcript was further confirmed by demonstration of the *Cac*8I-resistant species in the upper band PCR product (Figure 2). The F12/R12 PCR product cannot result from genomic contamination since it crosses introns 13 and 14.

Sequencing of the smaller RT-PCR product from PK9505 demonstrated a 58-bp deletion in the cDNA. The C to T mutation at nucleotide 2614 altered the dinucleotide GC (2613–2614) to GT resulting in the formation of a novel 5′ splice site within exon 14. As a consequence, there is aberrant, out-of-frame splicing at nucleotide 2612 to the exon 15 splice acceptor site (Figure 2) with a consequent frame shift to a stop codon eight residues downstream of the splice junction. It is significant that the splice variant does not restore the reading frame and therefore cannot potentially "rescue" the loss of function mutation in the genomic DNA. The single base change in the genomic sequence in family PK9505 resulted in

Table 2. PKD2 mutations and polymorphism[a]

Family	Exon	Sequence Change	Codon Change	Restriction Site
PK5147	4	Sub C→T 958	R320X	*Nla*III created
Oviedo 23	6	Del T 1443 or 1444 or 1445	fs 482→513X	
Family 9	6	Sub A→T 1532	D511V	*Bsp*EI lost[b]
PK5109	10	Del AT or TA 2021/2022 or 2022/2023 or 2023/2024	fs 675→681X	
PK9505	14	Sub C→T 2614	R872X and splice variant with fs 872→888X[c]	*Cac*8I lost
ADPKD4	14	Sub A→G 2657	Splice variant with fs 879→895X[d]	
Polymorphism	1	Sub G→A 420	G140G	*Bsu*361[e]

[a] sub, substitution; del, deletion; fs, frame shift.
[b] *Bsp*EI site is not a naturally occurring restriction site; it is introduced into wild-type sequence using a modified primer (Table 1).
[c] The mutation introduces a premature stop codon *and* also creates a splice donor site.
[d] The single base change results in an apparent missense change, D886G, based on the genomic sequence; however, analysis of reverse transcription-PCR products suggests that the pathogenic mutation is actually the splice variant shown and not the missense variant; hence, the latter is not shown in the table.
[e] The polymorphism does not alter a naturally occurring restriction site; the *Bsu*361 site is introduced into the more common allele, G, but not the less common allele, A, using a modified primer (Table 1).

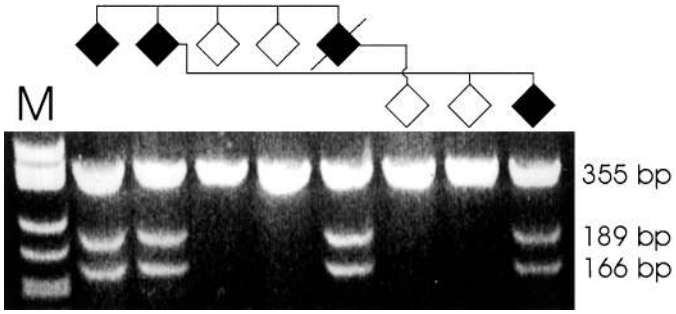

Figure 1. The mutation in family PK5147. The C to T transition at nucleotide 958 changes the sequence CA***C***G (nucleotides 956 to 959) to CA***T***G, thus introducing a novel *Nla*III restriction site. Digestion of the 355-bp exon 4 genomic PCR product (4) with *Nla*III shows segregation of the restriction site with the autosomal dominant polycystic kidney disease (ADPKD) phenotype in PK5147. M, marker lane.

the formation of three species of processed transcripts: a wild-type transcript, a transcript with a single base nonsense mutation, and an incorrectly spliced transcript with deletion and frame shift.

Frame Shifting Mutations

Two genomic mutations with deletion of one (family Oviedo 23) or two (PK5109) bases in exon sequences were identified (Table 2). Both mutations produce frame shifts with premature terminations. The deletion of a T in the trinucleotide 1443–1445 in exon 6 results in an altered reading frame at codon 482 with a termination at codon 513 (Figure 3). This mutation had previously been identified in two unrelated families (14). The current family, Oviedo 23, was ascertained in Spain, as was PK6533 in the previous report (14). Although there is no known relationship between these families, a common origin of these two mutations cannot be excluded by the present study. The dinucleotide deletion (of either AT or TA) in the dinucleotide pair at bases 2021–2024 in exon 10 results in a frame shift at codon 675 with a stop at codon 681 of the new reading frame (Figure 3). The latter is the first mutation reported in exon 10, leaving only exons 9 and 15 without reported mutations.

Missense Mutations

Two apparent missense variants were identified (Table 2). In the absence of a functional assay for PKD2, the conclusion that missense variants are pathogenic is inferential. Family 9 shows a single base change from A to T at nucleotide 1532 that introduces the nonconservative change of an aspartic acid residue at codon 511 to valine (D511V) in the predicted third transmembrane span of polycystin-2 (5). This aspartate is highly conserved in voltage-activated cation channel subunits, in both *Caenorhabditis elegans* PKD2 homologs (ZK945.9 and Y73F8A.B) (5) and in the PKD2-related PKD2L protein (6,7). This mutation demonstrates complete segregation with disease phenotype in family 9 (Figure 4) and was not identified in 101 normal chromosomes and 11 additional affected chromosomes examined.

Analysis of EBV-transformed lymphoblast RNA from the proband in ADPKD4 by RT-PCR with primers F12/R12 revealed the expected amplification product of 243-bp and a smaller product with reduced relative intensity (Figure 5). RT-PCR of normal lymphoblast RNA only produced the 243-bp product. Sequencing of the smaller product in ADPKD4 revealed a transcript with an out-of-frame 37-bp deletion. Amplification of the genomic segment from exon 14 to exon 15 with primers F17/R12 (Table 1) did not show evidence of a deletion (data not shown), suggesting that the smaller product resulted from aberrant splicing. Direct sequencing of the F17/R12 genomic PCR products (Table 1) iden-

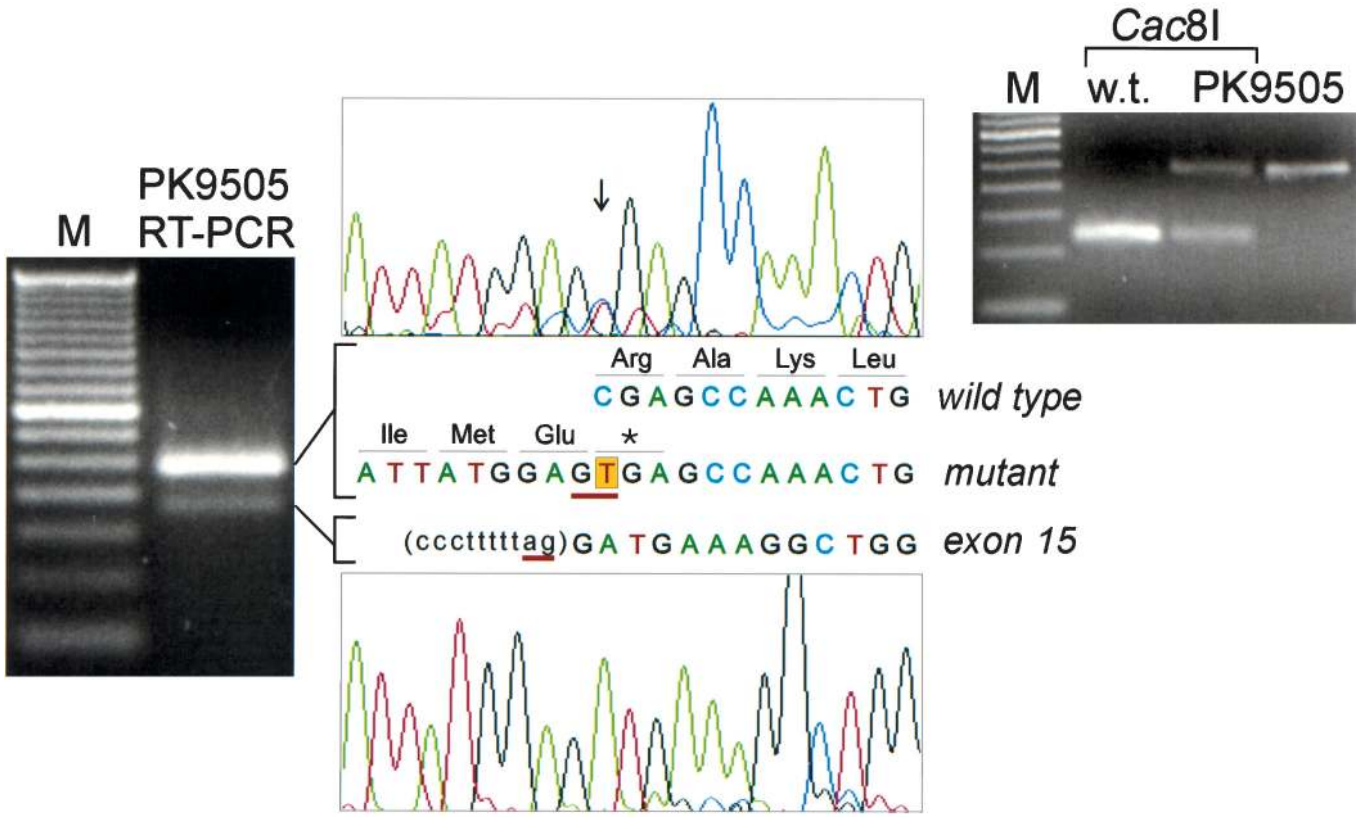

Figure 2. The mutation in family PK9505. The left panel shows reverse transcription (RT)-PCR products obtained with primers F12/R12. The upper band is the expected 243-bp size and the lower band is <200 bp (M, 50-bp ladder). The sequence of the upper band appears in the top tracing. The arrow indicates heterozygosity at nucleotide 2614. One transcript contains the wild-type sequence, and the other contains the mutant sequence with T substituted at nucleotide 2614, forming a TGA stop codon. The existence of two transcripts is confirmed by gel purification of the upper band followed by digestion with *Cac*8I (right panel). *Cac*8I (G***C***NNGC) cuts the wild-type (w.t.) completely, while the mutant PK9505 product is not cut by the enzyme; the uncut PK9505 starting product is shown in the far right lane. In addition, the mutation at nucleotide 2614 (C to T) forms a GT dinucleotide (underlined) that acts as a novel splice donor site. Sequencing of the smaller RT-PCR product (bottom electropherogram) shows that this processed transcript is the result of aberrant splicing of the novel donor site formed by the mutation to the wild-type splice acceptor site for exon 15 (4).

tified a change of A to G at nucleotide 2657. This mutation is predicted to encode a nonconservative change of aspartic acid to glycine at codon 886 (D886G) and occurs toward the middle of the 37-bp segment that is deleted in the lower band (Figure 5). Direct sequencing of the F17/R12 genomic PCR product in ADPKD4 family members demonstrated segregation of this mutation with the disease phenotype. Sequencing of all of exon 14, all of intron 14 (499 bp), and the coding portion of exon 15 did not reveal any other mutations in genomic DNA to account for the aberrant splicing (data not shown).

In contrast to the finding in PK9505, bidirectional sequencing of the gel-purified 243-bp (upper) RT-PCR product revealed only a single transcription product corresponding to the wild-type sequence. No mutant transcript with the single base change at position 2657 was found (Figure 5). The mutation at nucleotide 2657 activated a cryptic splice site 24 bases upstream of itself, at nucleotide 2633. Interestingly, this is not a consensus splice donor sequence. However, the mutant allele is exclusively processed as an aberrantly spliced, out-of-frame transcript without any of the missense product (Figure 5). The relative quantitative decrease in transcript intensity from the mutant allele likely results from decreased mRNA stability caused by the downstream stop codon (22). This is the second mutation identified in exon 14 (both in the current study) and is the most carboxyl mutation in *PKD2* described to date.

Polymorphisms

SSCA using exon 1b primers (4) identified a variant in one of the affected individuals as well as a healthy control subject. Sequencing revealed a G to A transition at nucleotide 420 that encoded a conservative change in a "wobble" base (GGG to GGA) for glycine. To test for this polymorphism directly, we introduced a two-base change into a PCR primer (Table 1) to engineer a *Bsu*36I restriction site (CCTNAG***G***, bold corresponds to G420) into PCR products amplified from the common allele, but not the variant allele. Seven of 40 (17.5%) normal chromosomes tested in this way did not have a G at position 420.

Polycystin-2 Protein Expression

An unresolved issue regarding all *PKD2* mutations detected in genomic and RT-PCR products is the true effect of these

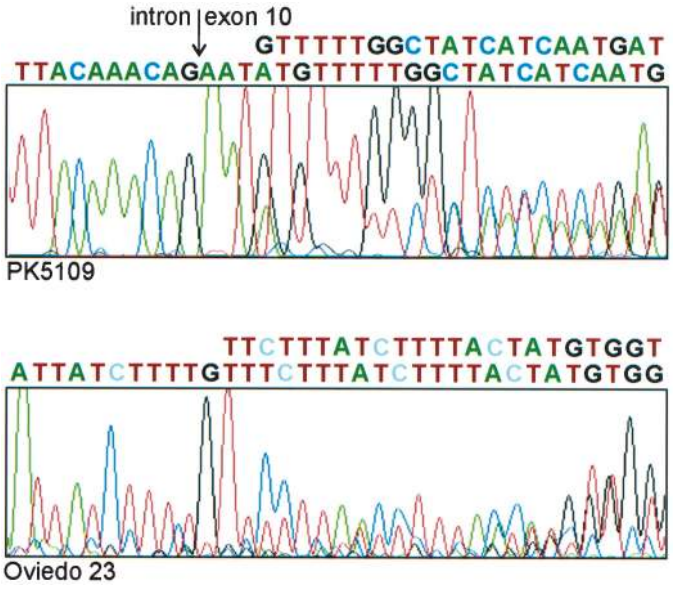

Figure 3. The mutations in PK5109 and Oviedo 23. The top electropherogram contains sequence of the IF18/IR15b exon 10 genomic PCR product (4) from family PK5109. The sequence contains the intron/exon 3′ splice site (arrow) with a deletion of an AT or TA dinucleotide within the exon resulting in a frame shift. The heterozygous nature of the genomic PCR product results in the dual peaks in the sequence after the deletion. The lower electropherogram shows exon 6 sequence obtained by from the IF2/IF8 genomic PCR product (4) in family Oviedo 23. Deletion of a single T in a T trinucleotide results in an altered reading frame with a downstream premature termination codon. The tracing again shows the heterozygous nature of the sequence downstream of the deletion.

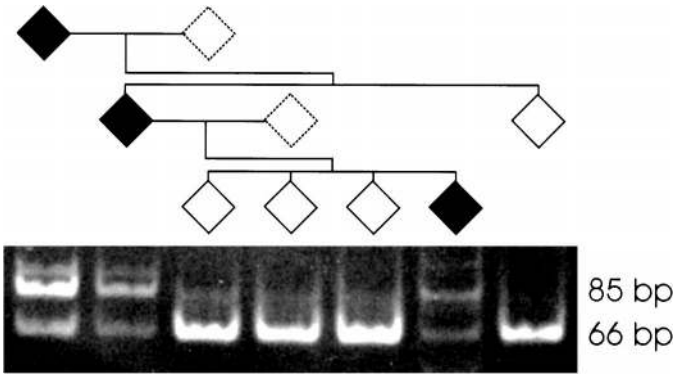

Figure 4. The mutation in family 9. The A to T change at nucleotide 1532 does not directly alter a restriction site. Therefore, we engineered a primer with a single nucleotide change that introduces a *Bsp*EI (5′TCCGG*A*3′, bold corresponds to A1532) restriction site into the wild-type allele (Table 1). The mutant allele does not form a *Bsp*EI site when amplified with this primer. The ethidium bromide-stained polyacrylamide gel shows that the 85-bp amplification product is completely digested to a 66-bp (and 19-bp, not visible) fragment in healthy individuals, whereas affected individuals in the family are heterozygous for the engineered *Bsp*EI site, confirming segregation of the mutation with the disease phenotype.

changes at the protein level. To begin to address questions regarding whether stable translation products are formed from mutant alleles, we analyzed expression of polycystin-2 by EBV-transformed lymphoblasts from affected and healthy individuals using a well-characterized anti-PKD2 antisera (Figure 6). Based on Northern data (5), the expected level of expression of PKD2 in lymphoblasts is lower than in other tissues.

Immunoblot analysis of lymphoblast membrane proteins using the YCC2 COOH-terminal antiserum identified an approximately 110-kD protein migrating identically to the band previously confirmed as polycystin-2 in mouse kidney (19). Several additional nonspecifically cross-reacting bands were also seen in lymphoblasts. We have shown previously that polycystin-2 is an Endo H-sensitive glycoprotein (Y. Cai, unpublished data), *i.e.*, digestion with Endo H results in a shift in electrophoretic mobility. Endo H treatment of lymphoblast membranes resulted in the predicted shift in mobility in the PKD2 band, confirming that the approximately 110-kD species identified in the lymphoblast membrane fraction was indeed polycystin-2.

In lanes loaded with equal amounts of total membrane protein, lymphoblasts from four patients with mutations in *PKD2* consistently showed reduction in normal polycysin-2 expression compared to unaffected ($n = 4$) or PKD1 patient ($n = 2$)-derived lymphoblast lines using either the YCC2 or YCB9 antisera (Figure 6). Translation products of *PKD2* cDNA with the PK9505 truncation mutation R872X introduced by site-directed mutagenesis can be detected in transiently transfected cells by both the COOH-terminal YCC2 antiserum and the NH_2-teminal YCB9 antiserum (data not shown). We did not detect any apparent truncation products in the ADPKD4 or the PK9505 lymphoblast lines using either antiserum under two different gel running conditions (Figure 6). These data suggest that in the lymphoblast lines from the PKD2 patients examined, there is little or no stable truncated mutant polycystin-2 protein expressed and there is no compensatory increase in transcription/translation of the normal PKD2 allele.

Discussion

The current study describes six mutations in *PKD2*, bringing to 43 the total number of mutations identified in the gene responsible for the second form of ADPKD. Only two of the previously described mutations have been investigated at the transcriptional level by RT-PCR. In one case, a single base insertion in a polyadenosine tract in exon 11 resulted in a frame shift that was identified in both genomic DNA and in RT-PCR product (13). In the second case, a 16-bp genomic deletion affecting the exon 2 splice acceptor site, no mutant transcript was identified (14). In the current study, we analyzed the genomic mutations and their consequences at the transcript level in two families. The mutations in families PK9505 and ADPKD4 occurred in exon 14 and are the two most COOH-terminal mutations described in *PKD2*. Each mutation was the result of a single base substitution. In PK9505, the single base change converted an arginine codon to a stop codon. Analysis of the transcripts in this patient showed that this mutation also

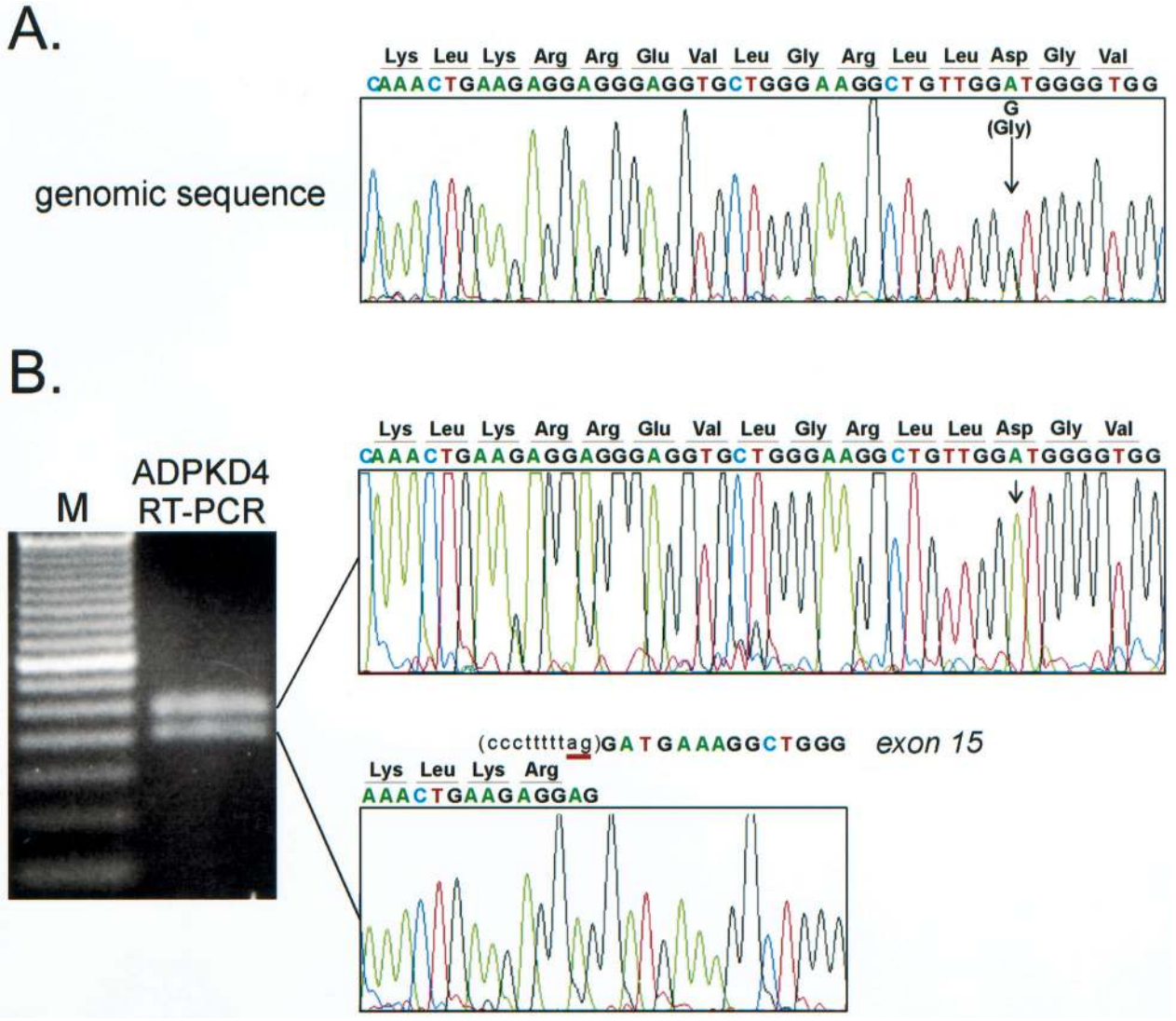

Figure 5. The mutation in family ADPKD4. (A) Sequencing of the genomic PCR product obtained with primers F17/R12 (Table 1) revealed an A to G transition in exon 14 at nucleotide 2657 as the only variation. This is predicted to change codon 879 from aspartic acid to glycine. (B) RT-PCR from a lymphoblast cell line of the proband in this family produced a doublet with primers F12/R12. Sequencing of the gel-purified upper band revealed only wild-type transcript (top electropherogram). Sequencing of the lower band showed aberrant splicing from nucleotide 2633 in exon 14 to the wild-type exon 15 splice acceptor site (lower electropherogram). Thus, a highly efficient cryptic splice donor site was activated 24 bp upstream of the mutation and resulted in a 37-bp splicing-induced deletion with consequent frame shift.

formed a potential cryptic splice donor site that spliced out of frame to the naturally occurring exon 15 splice acceptor sequence. This finding highlights the means by which the cell may escape even apparently unequivocally pathogenic mutations (23). Although not the case in this particular instance, the aberrant splicing could have occurred in frame. This would make it possible for the cell to produce a deleted, low-level transcript that could act as a hypomorphic allele with partial function and perhaps a variant phenotype. The truncated product resulting from the PK9505 mutation has been shown to lack the capacity to interact with the COOH terminus of PKD1 (10). Exon skipping, perhaps for the purposes of reading frame maintenance, can also be associated with stop codons in the skipped exons (24). We did not find exon skipping in this exon 14 mutation using RT-PCR primers from exons 13 and 15.

The single base change in ADPKD4 further highlights the importance of establishing the effects of genomic sequence variants at the transcriptional and, ultimately, translational, level (25). In this family, the mutation in the genomic DNA appears to be a nonconservative missense variant that may lead investigators to consider the functional importance of D886. However, analysis of the transcripts by RT-PCR reveals that this mutation results in the formation of a highly efficient cryptic splice site 24 bases upstream of the mutation itself. In contrast to the mutation in PK9505 where the major product is an admixture of the R872X and wild-type transcript, in ADPKD4 no transcript bearing the missense variant D886G is found. Recent studies on splicing have demonstrated that G triplets present in the interior of small vertebrate introns additively contribute to maximal splicing efficiency and spliceo-

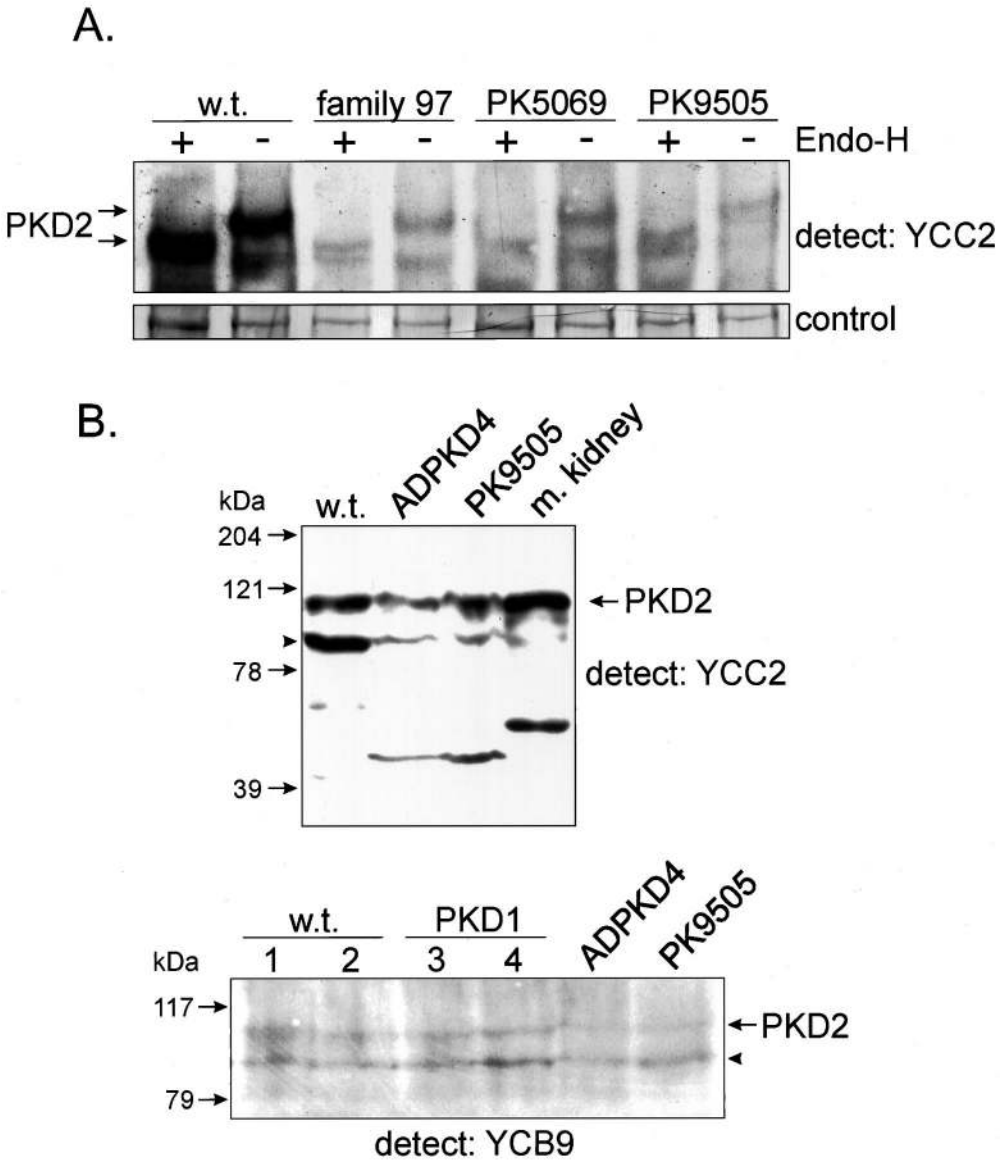

Figure 6. Immunoblotting of polycystin-2 from patient lymphoblast cell lines. (A) Polycystin-2 identified in total membrane protein fraction from patient lymphoblast cell lines using the YCC2 antiserum. The approximately 110-kD band (top arrow) shifts mobility after treatment with endoglycosidase H (Endo-H; lower arrow), confirming its identity with polycystin-2. The level of PKD2 expression in patient lymphoblast lines is reduced relative to wild type (w.t.). The mutations in family 97 (W380X) (5) and PK5069 (frame shift 180→212X) (14) have been reported previously. Even protein loading (20 μg on 8% sodium dodecyl sulfate-polyacrylamide gel electrophoresis [SDS-PAGE]) is indicated by Coomassie blue staining of the polyvinylidene difluoride membrane showing a approximately 200-kD band in the panel labeled control. (B) Absence of the predicted approximately 100-kD translation products of the mutant alleles in the two exon 14 mutant lymphoblast cell lines (ADPKD4, PK9505) as detected by the COOH-terminal YCC2 antiserum (20 μg protein, 8% SDS-PAGE; top panel) and the NH_2-terminal YCB9 antiserum (150 μg protein, 5% SDS-PAGE; bottom panel). Note that with both YCC2 and YCB9, the level of normal polycystin-2 expression is reduced in PKD2 lymphoblasts compared with wild type, whereas type 1 ADPKD patient-derived lymphoblasts have polycystin-2 expression comparable with wild type. The extraneous bands (arrowheads) migrate at approximately 90 kD and should not obscure the approximately 100-kD mutant bands in ADPKD4 and PK9505. m. kidney, mouse kidney; PKD1, type 1 ADPKD patient lymphoblast (unknown mutation) samples.

some assembly (26). These G triplets cause preferential utilization of 5′ (donor) splice sites upstream of the triplets themselves. The A to G change in ADPKD4 serves to form a G triplet in a region of exon 14 with two preexisting G triplets at nucleotides 2643–2645 and 2659–2661. The normal intron 14 is small (499 bp). This sequence alteration is apparently enough to mark the last 37 bases of exon 14 as intronic and cause the splicing machinery in the cell to utilize an upstream cryptic splice site that lacks a good consensus sequence. This example, as well as the finding that even silent genomic mutations can result in exon skipping (27), highlights the potentially complex consequences of simple base substitutions

in the ADPKD genes. It argues strongly for the need to study genomic sequence changes at the level of RNA transcripts in polycystic kidney disease (25).

Although the ADPKD4 mutation is instructive in a cautionary way, it is not proposed as a common mechanism for mutation. The family 9 mutation, D511V, likely represents a true missense variant. It is probably transcribed. In cell transfection studies, this mutant protein is stable and its subcellular distribution is indistinguishable from the wild-type, transfected expression product (Y. Cai, unpublished data). If a stable translation product is formed *in vivo*, it is most likely that this single amino acid change results in complete loss of polycystin-2 function since loss of function is required for cyst formation (17,19). Loss of function due to the D511V mutation is consistent with and supportive of the hypothesis that polycystin-2 is an ion channel subunit (5). Any mutation of the Asp residue, D258, in the K^+ channel S3 domain equivalent to D511 in the third transmembrane domain of polycystin-2 results in complete loss of the K^+ channel activity (28). This is not true of mutation to the other negatively charged residues in the K^+ channel S2 or S3 domains (28). The very high degree of conservation of this residue in polycystin-2 homologs through evolution from nematode to human is consistent with a critical functional importance for D511. The predicted antiparallel orientation of the third and fourth transmembrane segments in PKD2 suggests that the negatively charged D511 in the third transmembrane domain may form a charge pair with the positively charged K572 or K575 residues in fourth transmembrane span of polycystin-2 (5,28). In the K^+ or Ca^{2+} channels, these clusters of interacting charged residues within the membrane participate in voltage sensing.

Northern data suggest that the level of expression of *PKD2* in lymphoblasts is relatively low (5). In the current study, we were able to demonstrate that the polycystin-2 glycoprotein is detectable in immunoblots of lymphoblast membrane preparations. There is reduced expression of normal polycystin-2 in the type 2 ADPKD patient cell lines tested. This suggests that, at least in lymphoblast lines, germ-line inactivation of one allele of PKD2 results in reduced expression of polycystin-2 protein. We do not propose that this quantitative decrease in the protein product is pathogenic. However, if this quantitative variation can be demonstrated with consistency, then immunoblotting of lymphoblast membrane protein may be useful, in conjunction with clinical presentation and other diagnostic testing, in distinguishing PKD2 from PKD1. It is presently unknown whether the PKD2 protein product from the mutant allele is stable in patient tissues. Several truncated polycystin-2 polypeptides, including R872X, have been successfully expressed in cellular transfection systems (Y. Cai, unpublished data). We were unable to detect any truncated polycystin-2 in the lymphoblast cell lines of our two exon 14 truncation families. This suggests that *in vivo*, the mutant polypeptides may have diminished stability, at least in lymphoblast cell lines.

Intragenic polymorphisms in *PKD1* have proven critical to studies examining inactivation of the normal allele of the gene (17). Cyst formation in type 2 ADPKD is also likely to arise by a two-hit mechanism (19,29). To date, only one intragenic polymorphism in *PKD2* has been described (14). Its sequence basis is not known and it can only be assayed by SSCA, which has some degree of operator variability. In the current study, we define the first polymorphism in the coding sequence of *PKD2* and provide a PCR/restriction enzyme-based assay for the alleles. This and other intragenic *PKD2* polymorphisms will prove useful in human tissue studies examining the occurrence of second hits in *PKD2*.

We were able to identify mutations in 50% of families in our screening panel. These results are in keeping with previous studies (14) and reinforce the utility of SSCA mutation detection in *PKD2*. The spectrum of mutations we describe are also in keeping with those described previously for *PKD2*. In contrast to *PKD1*, to date no large-scale genomic deletions/rearrangements have been associated with the second gene for ADPKD. Among the mutations in *PKD2* identified thus far, several may prove to be very instructive in investigations of polycystin-2 function. Three of the mutations described in the current article, the two most COOH-terminal mutations in PKD2 and the missense variant in the third transmembrane domain, are likely to be among those most useful in such functional studies.

Acknowledgments

This work was supported by National Institutes of Health Grant R01DK48383 to Dr. Somlo. We thank Charles Query for helpful discussions, members of the ADPKD families for their participation in the study, George Grills for help with sequencing, and Vicente Torres, Patrick Parfrey, Currie Ahn, and Shigeo Horie for access to their family material.

References

1. Peters DJM, Sandkuijl LA: Genetic heterogeneity of polycystic kidney disease in Europe. In: *Contributions to Nephrology*: *Polycystic Kidney Disease*, edited by Breuning MH, Devoto M, Romeo G, Basel, Switzerland, Karger, 1992, pp 128–139
2. Parfrey PS, Bear JC, Morgan J, Cramer BC, McManamon PJ, Gault MH, Singh M, Hewitt R, Somlo Sl: The diagnosis and prognosis of autosomal dominant polycystic kidney disease. *N Engl J Med* 323: 1085–1090, 1990
3. Ravine D, Walker RG, Gibson RN, Forrest SM, Richards RI, Friend K, Sheffield LJ, Kincaid-Smith P, Danks DM: Phenotype and genotype heterogeneity in autosomal dominant polycystic kidney disease. *Lancet* 340: 1330–1333, 1992
4. Hayashi T, Mochizuki T, Reynolds DM, Wu G, Cai Y, Somlo S: Characterization of the exon structure of the polycystic kidney disease 2 gene (PKD2). *Genomics* 44: 131–136, 1997
5. Mochizuki T, Wu G, Hayashi T, Xenophontos SL, Veldhuisen B, Saris JJ, Reynolds DM, Cai Y, Gabow PA, Pierides A, Kimberling WJ, Breuning MH, Deltas CC, Peters DJM, Somlo S: *PKD2*, a gene for polycystic kidney disease that encodes an integral membrane protein. *Science* 272: 1339–1342, 1996
6. Nomura H, Turco AE, Pei Y, Kalaydjieva L, Schiavello T, Weremowicz S, Ji W, Morton CC, Meisler M, Reeders ST, Zhou J: Identification of PKDL, a novel polycystic kidney disease 2-like gene whose murine homologue is deleted in mice with kidney and retinal defects. *J Biol Chem* 273: 25967–25973, 1998

7. Wu GQ, Hayashi T, Park JH, Dixit MP, Reynolds DM, Li L, Cai Y, Coca-Prados M, Somlo S: Identification of the human PKD2-related cDNA, *PKD2L*: Tissue-specific expression and linkage mapping on chromosome 10q25. *Genomics* 54: 564–568, 1998
8. Moy GW, Mendoza LM, Schulz JR, Swanson WJ, Glabe CG, Vacquier VD: The sea urchin sperm receptor for egg jelly is a modular protein with extensive homology to the human polycystic kidney disease protein, PKD1. *J Cell Biol* 133: 809–817, 1996
9. Sandford R, Sgotto B, Aparicio S, Brenner S, Vaudin M, Wilson RK, Chissoe S, Pepin K, Bateman A, Chothia C, Hughes J, Harris PC: Comparative analysis of the polycystic kidney disease 1 (PKD1) gene reveals an integral membrane glycoprotein with multiple evolutionary conserved domains. *Hum Mol Genet* 6: 1483–1489, 1997
10. Qian F, Germino FJ, Cai Y, Zhang X, Somlo S, Germino GG: PKD1 interacts with PKD2 through a probable coiled-coil domain. *Nat Genet* 16: 179–183, 1997
11. Tsiokas L, Kim E, Arnould T, Sukhatme VP, Walz G: Homo- and heterodimeric interactions between the gene products of PKD1 and PKD2. *Proc Natl Acad Sci USA* 94: 6965–6970, 1997
12. Pei Y, He N, Wang K, Kasenda M, Paterson AD, Chan G, Liang Y, Roscoe J, Brissenden J, Hefferton D, Parfrey P, Somlo S, St. George-Hyslop P: A spectrum of mutations in the polycystic kidney disease-2 (PKD2) gene from eight Canadian kindreds. *J Am Soc Nephrol* 9: 1853–1860, 1998
13. Pei Y, Wang K, Kasenda M, Paterson AD, Liang Y, Huang E, Lian J, Rogovea E, Somlo S, St. George-Hyslop P: A novel frameshift mutation induced by an adenosine insertion in the polycystic kidney disease 2 (PKD2) gene. *Kidney Int* 53: 1127–1132, 1998
14. Veldhuisen B, Saris JJ, de Haij S, Hayashi T, Reynolds DM, Mochizuki T, Ellis R, Fossdal R, Bogdanova N, van Dijk MA, Coto E, Ravine D, Norby S, Verellen-Dumoulin C, Breuning MH, Somlo S, Peters DJM: A spectrum of mutations in the second gene for autosomal dominant polycystic kidney disease (PKD2). *Am J Hum Genet* 61: 547–555, 1997
15. Viribay M, Hayashi T, Telleria D, Mochizuki T, Reynolds DM, Alonso R, Lens XM, Moreno F, Harris PC, Somlo S, San Millan JL: Novel stop and frameshifting mutations in the autosomal dominant polycystic kidney disease 2 (PKD2) gene. *Hum Genet* 101: 229–234, 1997
16. Xenophontos SL, Constantinides R, Hayashi T, Mochizuki T, Somlo S, Pierides A, Deltas CC: A translation frameshift mutation induced by a cytosine insertion in the polycystic kidney disease 2 gene (PKD2). *Hum Mol Genet* 6: 949–952, 1997
17. Qian F, Watnick TJ, Onunchic LF, Germino GG: The molecular basis of focal cyst formation in human autosomal dominant polycystic kidney disease type I. *Cell* 87: 979–987, 1996
18. Brasier JL, Henske EP: Loss of the polycystic kidney disease (PKD1) region of chromosome 16p13 in renal cyst cells supports a loss-of-function model for cyst pathogenesis. *J Clin Invest* 99: 194–199, 1997
19. Wu G, D'Agati V, Cai Y, Markowitz G, Park JH, Reynolds DM, Maeda Y, Le TC, Hou H Jr, Kucherlapati R, Edelmann W, Somlo S: Somatic inactivation of Pkd2 results in polycystic kidney disease. *Cell* 93: 177–188, 1998
20. Watnick TJ, Torres VE, Gandolph MA, Qian F, Onuchic LF, Klinger KW, Landes G, Germino GG: Somatic mutation in individual liver cysts supports a two-hit model of cystogenesis in autosomal dominant polycystic kidney disease. *Mol Cell* 2: 247–251, 1998
21. Bear JC, McManamon P, Morgan J, Payne RH, Lewis H, Gault MH: Age at clinical onset and at ultrasonographic detection of adult polycystic kidney disease: Data for genetic counseling. *Am J Med Genet* 18: 45–53, 1984
22. Maquat LE: When cells stop making sense: Effects of nonsense codons on RNA metabolism in vertebrate cells. *RNA* 1: 453–465, 1995
23. Maquat LE: Defects in RNA splicing and the consequence of shortened translational reading frames. *Am J Hum Genet* 59: 279–286, 1996
24. Dietz HC, Kendzior RJJ: Maintenance of an open reading frame as an additional level of scrutiny during splice site selection. *Nat Genet* 8: 183–188, 1994
25. Cooper TA, Mattox W: The regulation of splice-site selection, and its role in human disease. *Am J Hum Genet* 61: 259–266, 1997
26. McCullough AJ, Berget SM: G triplets located throughout a class of small vertebrate introns enforce intron borders and regulate splice site selection. *Mol Cell Biol* 17: 4562–4571, 1997
27. Liu W, Qian C, Francke U: Silent mutation induces exon skipping of fibrillin-1 gene in Marfan syndrome. *Nat Genet* 16: 328–329, 1997
28. Planells-Cases R, Ferrer-Montiel AV, Patten CD, Montal M: Mutation of conserved negatively charged residues in the S2 and S3 transmembrane segments of a mammalian K+ channel selectively modulates channel gating. *Proc Natl Acad Sci USA* 92: 9422–9426, 1995
29. Koptides M, Hadjimichael C, Koupepidou P, Pierides A, Constantinou DC: Germinal and somatic mutations in the PKD2 gene of renal cysts in autosomal dominant polycystic kidney disease. *Hum Mol Genet* 8: 509–513, 1999